Editor: Dietrich Stauffer, stauffer@thp.uni-koeln.de
Muhammad Sahimi, moe@iran.usc.edu

New Computational Approaches to the Analysis of Interbeat Intervals in Human Subjects

By Mohammad Reza Rahimi Tabar, Fatemeh Ghasemi, Joachim Peinke, Rudolf Friedrich, Kamran Kaviani, Fatemeh Taghavi, Sara Sadeghi, Golnoosh Bizhani, and Muhammad Sahimi

COMPLEX, SELF-REGULATING SYSTEMS SUCH AS THE HUMAN HEART MUST PROCESS INPUTS WITH A BROAD RANGE OF CHARACTERISTICS TO GENERATE PHYSIOLOGICAL data and time series.[1–3] Many of these physiological time series seem to be highly chaotic, represent nonstationary data, and fluctuate in an irregular and complex manner. One hypothesis is that the seemingly chaotic structure of physiological time series arises from external and intrinsic perturbations that push the system away from a homeostatic set point. An alternative hypothesis is that the fluctuations are due, at least in part, to the system's underlying dynamics.

In this review, we describe new computational approaches—based on new theoretical concepts—for analyzing physiological time series. We'll show that the application of these methods could potentially lead to a novel diagnostic tool for distinguishing healthy individuals from those with congestive heart failure (CHF).

Physiological Time Series

Recent research suggests that physiological time series can possess fractal and self-similar properties, which are characterized by the existence of long-range correlations (with the correlation function being a power-law type). However, until recently, the analysis of such fluctuations' fractal properties was restricted to computing certain characteristics based on the second moment of the data, such as the power spectrum and the two-point autocorrelation function. These analyses indicated that the fractal behavior of healthy, free-running physiological systems could be characterized, at least in some cases, by $1/f$-like scaling of the power spectra over a wide range of time scales.[4,5] A time series that exhibits such long-range correlations with a power-law correlation function and is also homogeneous (different parts of the series have identical statistical properties) is called a *monofractal* series.

However, many physiological time series are inhomogeneous in the sense that distinct statistical and scaling properties characterize different parts of the series. In addition, there is some evidence that physiological dynamics can exhibit nonlinear properties.[6–12] Such features are often associated with *multifractal* behavior—the presence of long-range power-law correlations in the higher moments of the time series—which, unlike monofractals, are nonlinear functions of the second moment's scaling exponents.[13] Up until recently, though, robust demonstration of multifractality of nonstationary time series was hampered by problems related to significant bias in the estimates of the data's singularity spectrum, due to the time series' diverging negative moments. A new wavelet-based multifractal formalism helps address such problems.[13]

Among physiological time series, the study of the statistical properties of heartbeat interval sequences has attracted much attention.[14–17] The interest is at least partly due to the facts that

- the heart rate is under direct neuroautonomic control;
- interbeat interval variability is readily measured by noninvasive means; and
- analysis of heart-rate dynamics could provide important diagnostic and prognostic information.

Thus, extensive analysis of interbeat interval variability represents an important quantity for elucidating possibly nonhomeostatic physiological variability.

Figure 1 shows examples of cardiac interbeat time series (the output of a spatially and temporally integrated neuroautonomic control system) for healthy individuals and those with CHF. In the conventional approaches to analyzing such data, we would assume the apparent noise has no meaningful structure, so we wouldn't expect to gain any un-

 Copublished by the IEEE CS and the AIP 1521-9615/06/$20.00 © 2006 IEEE

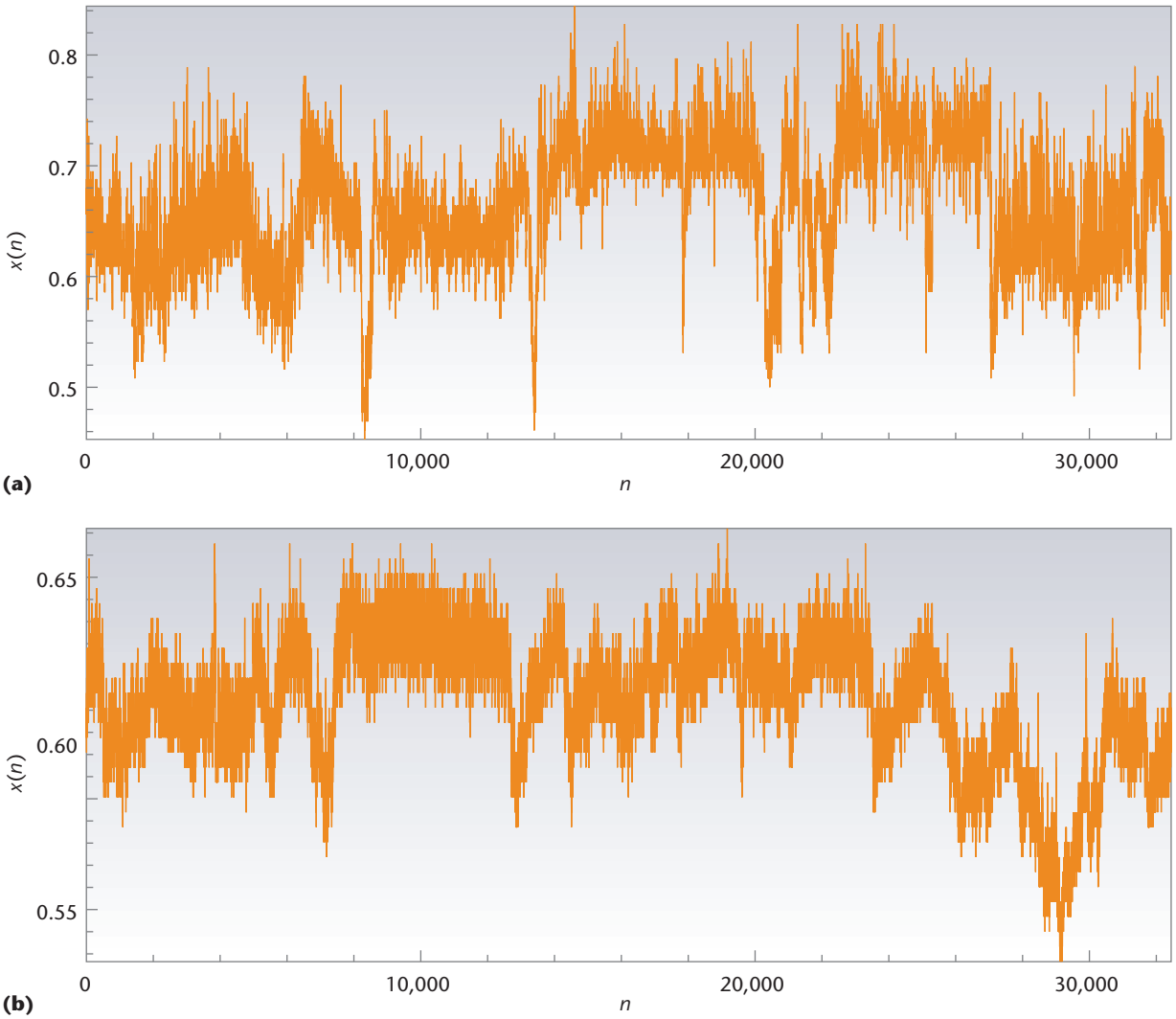

Figure 1. Cardiac interbeat time series. The (a) interbeat fluctuations of healthy subjects and (b) those with congestive heart failure differ greatly (note the erratic fluctuations and patchiness).

derstanding of the underlying system through the study of such fluctuations. Conventional studies that focus on averaged quantities therefore usually ignore these fluctuations—in fact, they're often labeled as noise to distinguish them from the true time series of interest.

However, by adapting and extending methods developed in modern statistical physics and nonlinear dynamics, the physiological fluctuations in Figure 1 can be shown to exhibit an unexpected hidden scaling structure.[5,10,13,18,19] Moreover, the fluctuation dynamics and associated scaling features can change with pathological perturbation. These discoveries have raised the possibility that understanding the origin of such temporal structures and their alterations through disease could elucidate certain basic aspects of heart-rate control mechanisms and increase the potential for clinical monitoring.

But despite this considerable progress, several interesting features must still be analyzed and interpreted. The theoretical concepts we discuss here are based on the possible Markov properties of the time series; a cascade of information from large time scales to small ones that are built based on *increments* in the time series; and the extended self-similar properties of the beat-to-beat fluctuations of healthy subjects as well as those with CHF. The method we describe uses a set of data for a given phenomenon that contains a degree of stochasticity and numerically constructs a relatively simple equation that governs the phenomenon. In addition to being accurate, this method is quite general, can provide a rational explanation for complex features of the phenomenon under study, and requires no scaling feature or assumption.

As we analyze cardiac interbeat intervals, we'll also look at new methods for computing the Kramers-Moyal (KM) coefficients for the increments of interbeat intervals fluctu-

ations, $\Delta x(\tau) = [x(t + \tau) - x(t)]/\sigma_\tau$, where σ_τ is the standard deviation of increments in the interbeat data. Whereas the first and second KM coefficients (representing the drift and diffusion coefficients in a Fokker-Planck [FP] equation) have well-defined values, the third- and fourth-order KM coefficients might be small. If so, we can numerically construct an FP evolution equation for the *probability density function* (PDF), $P(\Delta x, \tau)$, which, in turn, can be used to gain information on the PDF's evolution as a function of the time scale τ.[20–23]

Regeneration of Stochastic Processes

Let's start by examining the computations that lead to the numerical construction of a stochastic equation. This equation describes the phenomenon that generates the data set, which is then used to reconstruct the original time series. Two basic steps are involved in the numerical analysis of the data and their reconstruction.

Data Examination

We must first examine the data to see whether they follow a Markov chain and, if so, we estimate the Markov time scale t_M. As is well known, a given process with a degree of stochasticity can have a finite or an infinite Markov time scale, which is the minimum time interval over which the data can be considered to be a Markov process.[20,24] To determine the Markov scale t_M, we note that a complete characterization of the stochastic fluctuations of $x(t)$ requires the numerical evaluation of the joint PDF $P_n(x_1, t_1; \cdots; x_n, t_n)$ for an arbitrary n, which is the number of data points in the time series $x(t)$. If this time series is a Markov process, we can make an important simplification because P_n, the n-point joint PDF, is generated by the product of the conditional probabilities $P(x_{i+1}, t_{i+1} \mid x_i, t_i)$ for $i = 1, \cdots, n - 1$. A necessary condition for $x(t)$ to be a Markov process is that the Chapman-Kolmogorov (CK) equation,

$$P(x_2, t_2 \mid x_1, t_1) = \int \mathrm{d}(x_3) P(x_2, t_2 \mid x_3, t_3) P(x_3, t_3 \mid x_1, t_1), \qquad (1)$$

holds for any value of t_3 in the interval $t_2 < t_3 < t_1$. We can check the CK equation's validity for various x_1 by comparing the directly computed conditional probability distributions $P(x_2, t_2 \mid x_1, t_1)$ with the ones computed according to the right side of Equation 1. The simplest way to determine t_M for stationary or homogeneous data is the numerical computation of the quantity $S = |P(x_2, t_2 \mid x_1, t_1) - \int \mathrm{d}x_3\, P(x_2, t_2 \mid x_3, t_3) P(x_3, t_3 \mid x_1, t_1)|$ for a given x_1 and x_2, in terms of, for example, $t_3 - t_1$ (taking into account the possible numerical errors in estimating S). Then, $t_M = t_3 - t_1$ for that value of $t_3 - t_1$, for which S vanishes or is nearly zero (achieves a minimum).

Numerical Construction

Numerical construction of an effective stochastic equation that describes the fluctuations of the quantity $x(t)$, representing the time series, constitutes the second step. The CK equation yields an evolution equation for the PDF $P(x, t)$ across the scales t. The CK equation, when formulated in differential form, yields a master equation that takes the form of an FP equation:

$$\frac{\partial}{\partial t} P(x,t) = \left[-\frac{\partial}{\partial x} D^{(1)}(x,t) + \frac{\partial^2}{\partial dx^2} D^{(2)}(x,t) \right] P(x,t) \ . \qquad (2)$$

We can compute the drift and diffusion coefficients, $D^{(1)}(x, t)$ and $D^{(2)}(x, t)$, directly from the data and the moments $M(k)$ of the conditional probability distributions

$$D^{(k)}(x,t) = \frac{1}{k!} \lim_{\Delta t \to 0} M^{(k)} \ , \qquad (3)$$

$$M^{(k)} = \frac{1}{\Delta t} \int dx'(x' - x)^k P(x', t + \Delta t \mid x, t) \ . \qquad (4)$$

Note that the FP formulation is equivalent to the following Langevin equation:

$$\frac{d}{dt} x(t) = D^{(1)}(x) + \sqrt{D^{(2)}(x)}\, f(t) \ , \qquad (5)$$

where $f(t)$ is a *random force* with zero mean and Gaussian statistics, δ-correlated in t—that is, $\langle f(t) f(t') \rangle = 2\delta(t - t')$. Note that the numerical reconstruction of a stochastic process doesn't imply that the data don't contain any correlations or that Equations 2 through 5 ignore the correlations.

Equation 5 enables us to *reconstruct* a stochastic time series $x(t)$, which is similar to the original one in the statistical sense. The stochastic process $x(t)$ is regenerated by iterating Equation 5, which yields a series of data without memory. To compare the regenerated series with the original $x(t)$, we must take the temporal interval in the numerical discretization of Equation 5 to be unity (or renormalize it to unity, if need be). However, the Markov time is typically greater than unity, so we correlate the data over the Markov time scale t_M, for which there are several methods.[21,22,25] A new tech-

nique that we've used in our own studies, which we refer to as the *kernel method*, considers a kernel function $K(u)$ that satisfies the condition

$$\int_{-\infty}^{\infty} K(u)du = 1\,, \tag{6}$$

such that the data are determined, or reconstructed, by

$$x(t) = \frac{1}{nh}\sum_{i=1}^{n} x(t_i)K\left(\frac{t-t_i}{h}\right), \tag{7}$$

where h is the window width. One of the most accurate kernels is the standard normal density function, $K(u) = (2\pi)^{-1/2}\exp(-1/2u^2)$. In essence, the kernel method represents the time series as a sum of "bumps" placed at the "observation" points, with its kernel determining the shape of the bumps and its window width h fixing their width. It's evident that, over the scale h, the kernel method correlates the data.

Analysis of Fluctuations in Human Heartbeats

To show how the reconstruction method is used in practice, we've applied the method to reconstruct the fluctuations found in the heartbeats of both healthy and ill human subjects by taking $h \simeq t_M$. Recent studies[5,19,26,27] reveal that under normal conditions, beat-to-beat fluctuations in heart rates might display extended correlations of the type typically exhibited by dynamical systems far from equilibrium. Some have argued,[26] for example, that the various stages of sleep might be characterized by extended correlations of heart rates separated by a large number of beats. Although the existence of extended correlations in the fluctuations of human heartbeats is an interesting and important result, we argue that the Markov time scale t_M and the associated drift and diffusion coefficients of the interbeat fluctuations of healthy subjects and those with CHF can help us better distinguish the two classes of subjects, particularly in the early stages of the disease, because these quantities have completely different behaviors for the two classes of patients.

We've used this method to analyze both daytime (12:00 p.m. to 18:00 p.m.) and nighttime (12:00 a.m. to 6:00 a.m.) heartbeat time series of healthy subjects, and the daytime records of patients with CHF.[28,29] The database included 10 healthy subjects (seven females and three males aged between 20 and 50, with an average age of 34.3 years) and 12 subjects with CHF (three females and nine males aged between 22 and 71, with an average age of 60.8 years). Figure 1 presents the typical data.

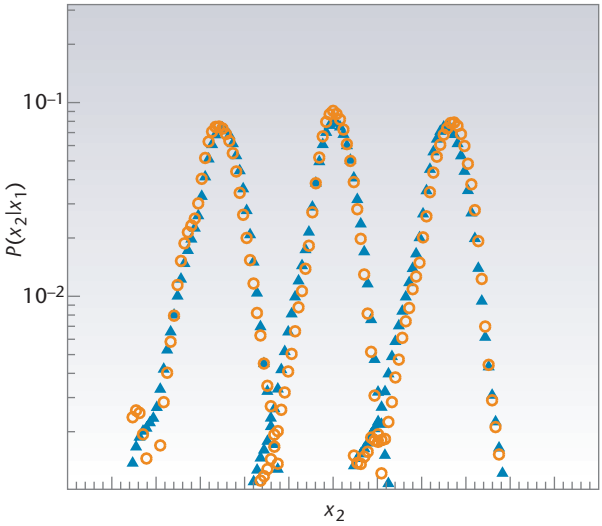

Figure 2. Test of Chapman-Kolmogorov equation for x_1 = –5, x_1 = 0, and x_1 = 5. Solid and open symbols represent the directly evaluated probability density function (PDF) and the integrated PDF. The PDFs are shifted in the vertical directions for better presentation, and values of x are measured in units of the standard deviation.

As the first step of the analysis, we compute the data's Markov time scale t_M. From the daytime data for healthy subjects, t_M = 3, 3, 3, 1, 2, 3, 3, 2, 3, and 2 (all values are measured in units of the average time scale for each subject's beat-to-beat times). The corresponding values for the nighttime records are 3, 3, 1, 3, 3, 2, 3, 3, 2, and 3, respectively, comparable to those for daytime. However, for CHF patients' daytime records, the computed Markov time scales are 151, 258, 760, 542, 231, 257, 864, 8, 366, 393, 385, and 276. Therefore, the healthy subjects are characterized by much smaller t_M values than those of the CHF patients, giving us an unambiguous quantity for distinguishing the two classes of patients.

Next, we check the CK equation's validity for describing the phenomenon for several x_1-triplets by comparing the directly computed conditional probability distributions $P(x_2, t_2 | x_1, t_1)$ with the ones computed according to the right side of Equation 1. Here, x is the interbeat, and we define, $x \equiv (x - \bar{x})/\sigma$ for all samples, where $\bar{x}$ and σ are the interbeat data's mean and standard deviations. Figure 2 compares the two PDFs computed by the two methods. Assuming the statistical errors to be the square root of the number of events in each bin, the two PDFs are *statistically* identical.

Figure 3 shows the corresponding drift and diffusion coefficients, $D^{(1)}(x)$ and $D^{(2)}(x)$, demonstrating that in addition to the Markov time scale t_M, the two coefficients provide another important indicator for distinguishing the ill subjects

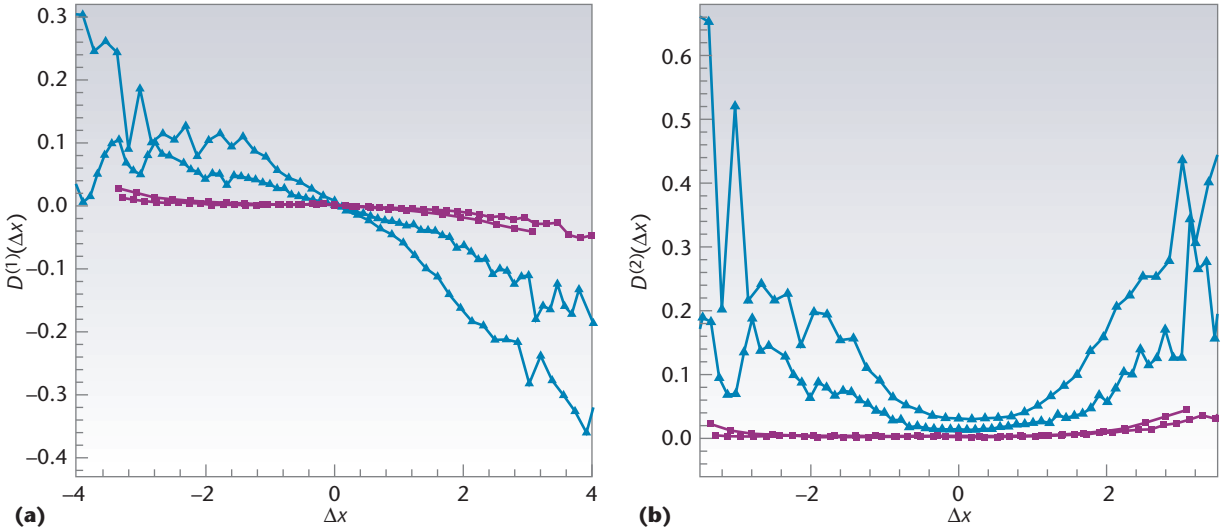

Figure 3. The drift and diffusion coefficients, $D^{(1)}(x)$ and $D^{(2)}(x)$, estimated by Equation 3. For the healthy subjects (triangles), $D^{(1)}(x)$ and $D^{(2)}(x)$ follow linear and quadratic behavior in x, whereas for patients with congestive heart failure (squares), they follow third- and fourth-order polynomials in x.

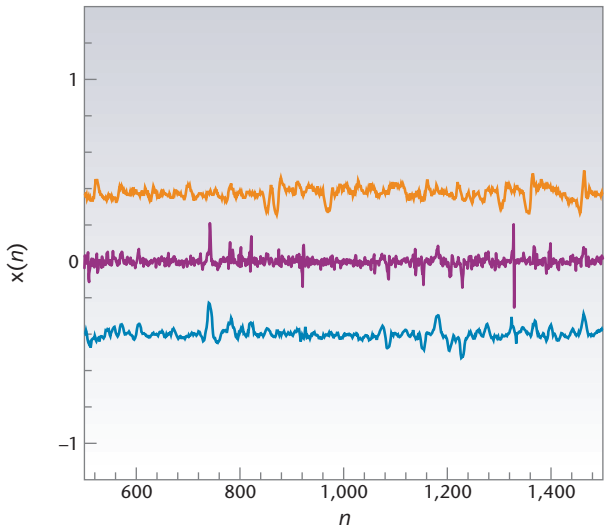

Figure 4. Reconstructed time series. The actual interbeat data for a healthy subject (top), the regenerated data (middle) using the corresponding Langevin equation, and the regenerated data using the kernel method (bottom). For better representation, the time series are shifted in the vertical directions.

from the healthy ones. For the healthy subjects, the drift $D^{(1)}$ and the diffusion coefficients $D^{(2)}(x)$ follow (approximately) linear and quadratic functions of x, respectively, whereas the corresponding coefficients for patients with CHF follow (approximately) third- and fourth-order equations in x. Thus, for the healthy subjects,

$$D^{(1)}(x) = -0.12x, \tag{8}$$

$$D^{(2)}(x) = (5 - 4.2x + 7x^2) \times 10^{-2}, \tag{9}$$

whereas for the patients with CHF,

$$D^{(1)}(x) = -(26x + 18x^2 + 7x^3) \times 10^{-4}, \tag{10}$$

$$D^{(2)}(x) = (6 - 7x + 5x^2 + 3x^3 + 2x^4) \times 10^{-4}, \tag{11}$$

which Kuusela also obtained.[29] For other databases measured for other patients, the functional dependence of $D^{(1)}$ and $D^{(2)}(x)$ would be the same, but with different numerical coefficients, and the coefficients' order of magnitude would be the same for all healthy subjects and likewise for those with CHF.[20] Moreover, if we analyze different parts of the time series separately, we find practically the same Markov time scale for different parts of the time series, but with some differences in the numerical values of the drift and diffusion coefficients. These coefficients have the same *functional forms*, but with different coefficients in equations such as Equations 8 through 11. Hence, we can distinguish the data for nighttime from those patients when they are awake.

There is yet another important difference between the heartbeat dynamics of the two classes of subjects: compared with the healthy subjects, the drift and diffusion coefficients for CHF patients are very small, reflecting, in some sense, their large Markov time scale t_M. Large Markov times imply longer correlation lengths for the data, and it's well known that the diffusivity in correlated system is smaller

than those in random ones. Hence, we can use the Markov time scales—and the dependence of the drift and diffusion coefficients on x, as well as their comparative magnitudes—to characterize the dynamics of human heartbeats and their fluctuations, and to distinguish healthy subjects from those with CHF.

But how accurate is the reconstruction method? Figure 4 shows a comparison between the original time series $x(n)$ and those reconstructed by the Langevin equation (using, for example, Equations 5, 8, and 9) and the kernel method. Although both methods generate series that look similar to the original data, the kernel method appears to better mimic the original data's behavior. To demonstrate Equation 7's accuracy, Figure 5 compares the second moment of the stochastic function, $C_2(m) = \langle [x(0) - x(m)]^2 \rangle$, for both the measured and reconstructed data by using the kernel method. The agreement between the two is excellent, but such agreement isn't sufficient for proving a reconstruction method's accuracy, so we also checked the accuracy of the reconstructed higher-order structure function, $S_n = \langle | x(t_1) - x(t_2) |^n \rangle$.[28,29] We found the agreement between S_n for the original and reconstructed time series for $n \leq 5$ to be excellent while the difference between higher-order moments of the two times series increases.

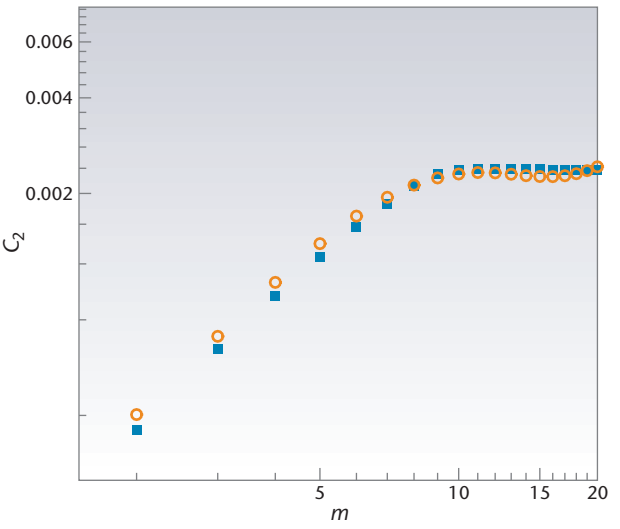

Figure 5. Logarithmic plot of Figure 4. For the second moment of the height-difference versus *m*, circles represent the actual data, and squares represent the samples regenerated by the kernel method.

A Cascade of Information

We could argue that if long-range, *nondecaying* correlations exist in the time series, we might not be able to use the reconstruction method for analyzing them because the correlations in a Markov process decay exponentially. Aside from the fact that the method we've described provides an unambiguous way of distinguishing healthy subjects from those with CHF in such cases, which we believe is more effective than simply analyzing the data to see what type of correlations might exist in the data, we argue that nondecaying correlations do not, in fact, pose any limitations to the reconstruction method's fundamental ideas and concepts.

The reason why is that even if the reconstruction method fails to describe long-range, nondecaying correlations in the data, we can still use the same method to analyze the data by invoking an important result recently pointed out by several groups.[20,21,23–25] They studied the evolution of the PDF of several stochastic properties for turbulent free jets along with rough surfaces. They argued that the conditional PDF of a stochastic field's increments, such as the increments in the turbulent flow's velocity field or a rough surface's height fluctuations, satisfies the CK equation even if the velocity field or the height function itself contains long-range, nondecaying correlations. This enabled them to derive an FP equation for describing the systems under study, giving us a way of analyzing correlated stochastic time series or data in terms of the corresponding FP and CK equations. We now describe the conditions under which such a formulation can be used.

In such cases, we compute the KM coefficients for the increments of the interbeat intervals' fluctuations, $\Delta x(\tau) = x(t + \tau) - x(t)$, rather than the time series $x(t)$ itself. We then check whether the first and second KM coefficients that represent the drift and diffusion coefficients in an FP equation have well-defined and finite values when the third- and fourth-order KM coefficients are small. According to Pawula's theorem,[24] the KM expansion,

$$\frac{\partial}{\partial t} P(x,t \mid x_0,t_0) = \sum_{k=1}^{\infty} \left(-\frac{\partial}{\partial x} \right)^k \left[D^{(k)}(x,t) P(x,t \mid x_0,t_0) \right], \quad (12)$$

can be truncated after the second (diffusive) term, provided that the third- and fourth-order coefficients $D^{(4)}$ vanishes, or are very small compared with the first two coefficients. If so—and this is often the case—the KM expansion, Equation 12, reduces to an FP evolution equation. In this case, an FP equation is numerically constructed by computing its drift and diffusion coefficients for the PDF $P(\Delta x, \tau)$, which, in turn, is used to gain information on the PDF shape's evolution as a function of the time scale τ. In essence, if the first two KM coefficients have numerically meaningful values

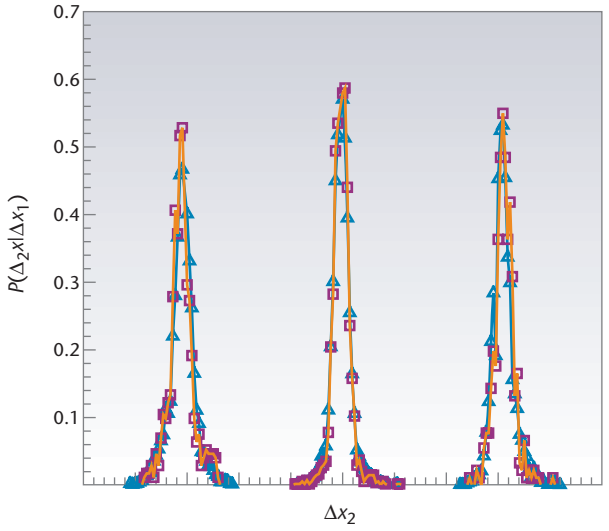

Figure 6. Test of Chapman-Kolmogorov equation for $\Delta x_1 = -0.42$, $\Delta x_1 = 0$, and $\Delta x_1 = 0.42$. The solid and open symbols represent the directly evaluated probability density function (PDF) and the one obtained from Equation 1. The PDFs are shifted in the horizontal directions for clarity. Values of Δx are measured in units of the standard deviation of the increments, and the time scales τ_1, τ_2, and τ_3 are 10, 30, and 20.

(that is, they aren't very small), and the third and higher coefficients are small compared to the first two coefficients, we can use the previously described reconstruction method—Equations 2 through 5—for the increments of the times series, rather than the time series itself.

Therefore, performing the same type of computations as described earlier but for the increments $\Delta x(t)$, we can compute the following results for the healthy subjects,[28]

$$D^{(1)}(\Delta x, \tau) = -(3\Delta x + 0.46) \times 10^{-2}, \quad (13)$$

$$D^{(2)}(\Delta x, \tau) = [(1 + 11\tau^{-1})(\Delta x)^2 + (5.7 + 28.7\tau^{-1})] \times 10^{-2}, \quad (14)$$

whereas for the CHF patients, we obtain

$$D^{(1)}(\Delta x, \tau) = -(1.3\Delta x + 0.18) \times 10^{-2}, \quad (15)$$

$$D^{(2)}(\Delta x, \tau) = [(5 + 5\tau^{-1})(\Delta x)^2 + (13 + 66\tau^{-1})] \times 10^{-3}. \quad (16)$$

Estimates of these coefficients are less accurate for large values of Δx; we also compute the average of the coefficients $D^{(1)}$ and $D^{(2)}$ for the entire set of healthy subjects, as well as those with CHF. Moreover, $D^{(4)}$ is approximately $1/10D^{(2)}$ for the healthy subjects and roughly $1/20D^{(2)}$ for those with CHF. Therefore, the KM expansion can indeed be truncated beyond the second term, and the FP formulation is numerically justified.

Equations 13 through 16 state that the drift coefficients for the healthy subjects and those with CHF have the same order of magnitude, whereas the diffusion coefficients for the given τ and Δx differ by roughly one order of magnitude. This points to a relatively simple way of distinguishing the two classes of subjects. Moreover, the τ-dependence of the diffusion coefficient for the healthy subjects is stronger than that of those with CHF (in the sense that the numerical coefficients of τ^{-1} are larger for the healthy subjects; see Figures 7 and 8). Note that these results are consistent with those presented earlier for the time series $x(t)$ itself—that is, they distinguish the two classes of patients through their different drift and diffusion coefficients. Figure 6 compares the directly computed PDFs with those obtained using Equation 1.

The healthy subjects' strong τ-dependence in the diffusion coefficient $D^{(2)}$ indicates that the nature of the PDF of their increments Δx for given τ—that is, $P(\Delta x, \tau)$—is intermittent and that its shape should change strongly with τ. However, for CHF patients, the PDF isn't so sensitive to the change of the time scale τ, thus indicating that the increments' fluctuations for these patients aren't intermittent.

Extended Self-Similarity of Interbeat Intervals

Let's look at another computational method for distinguishing healthy subjects from CHF patients. The method is based on the concept of *extended self-similarity* (ESS) of a time series. This concept is particularly useful if the time series for interbeat fluctuations (or other types of time series) don't, as is so often the case, exhibit scaling over a broad interval. In such cases, the time interval in which the structure function of the time series,

$$S_q(\tau) = \langle |x(t + \tau) - x(t)|^q \rangle, \quad (17)$$

behaves as

$$S_q(\tau) \sim \tau^{\xi q}, \quad (18)$$

is small, in which case the existence of scale invariance in the data can be questioned. Instead of rejecting outright the existence of scale invariance, we must first explore the possibility of the data having scale invariance via the concept of ESS.

The ESS is a powerful tool for checking data's non-Gaussian properties,[30–32] and researchers have used it extensively in turbulent-flow studies. Indeed, when analyzing the interbeat time series for human subjects (and other types

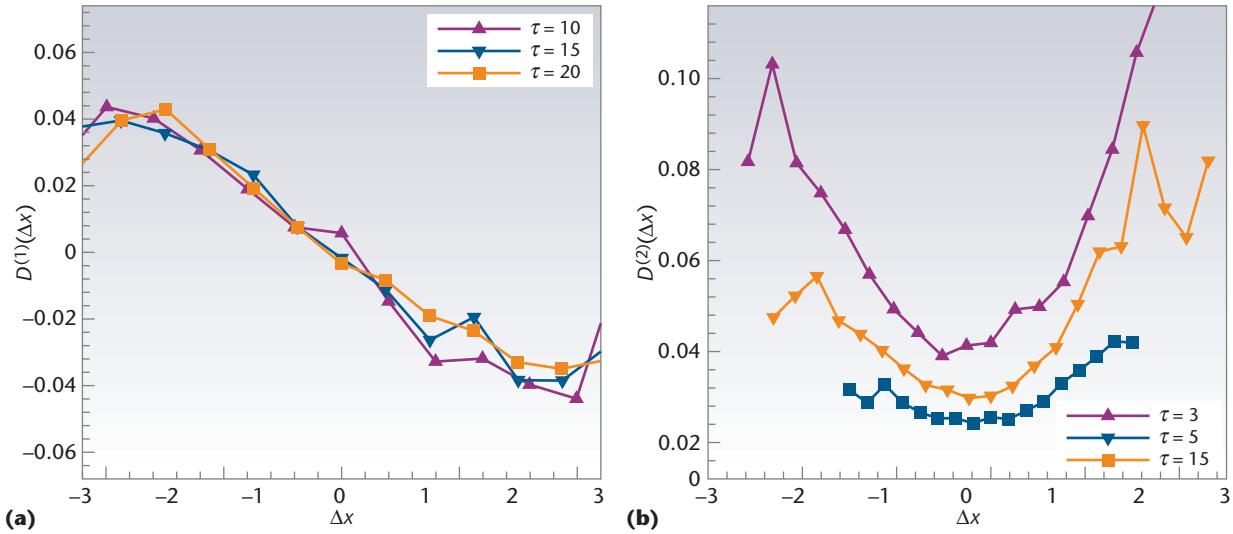

Figure 7. Drift and diffusion coefficients, $D^{(1)}(\Delta x)$ and $D^{(2)}(\Delta x)$. Estimated from Equation 3 for a healthy subject, these coefficients follow roughly linear and quadratic relations, respectively.

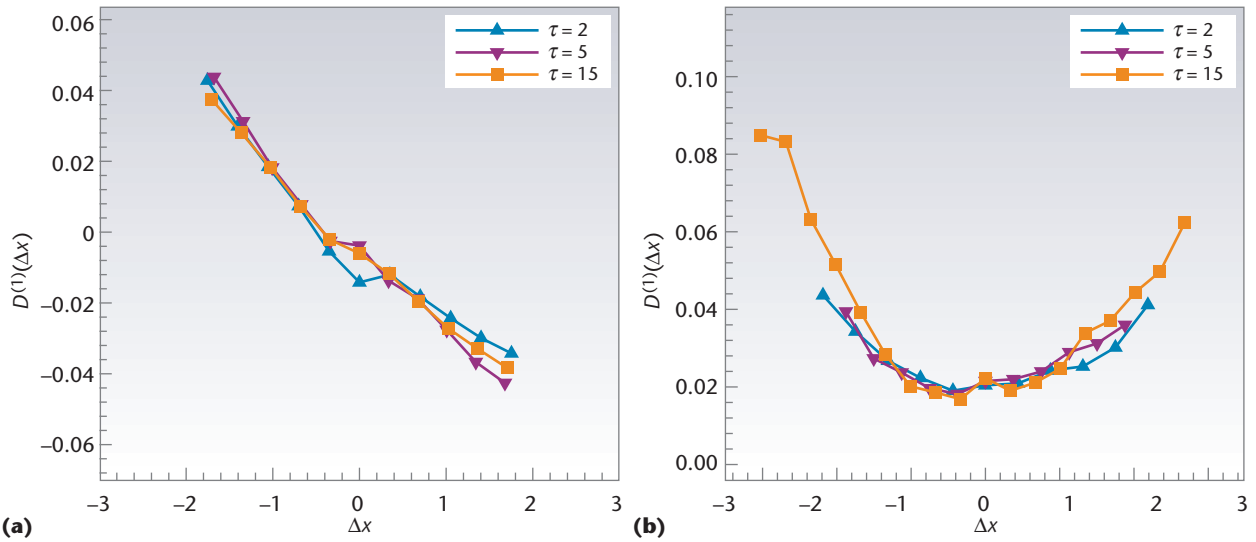

Figure 8. Drift and diffusion coefficients, $D^{(1)}(\Delta x)$ and $D^{(2)}(\Delta x)$. Estimated from Equation 3 for patients with congestive heart failure, they follow roughly linear and quadratic behavior, respectively.

of time series), we can, in addition to the structure function's τ-dependence, compute a generalized form of scaling using the ESS concept. In many cases, when the structure functions $S_q(\tau)$ are plotted against a specific order's structure function—say, $S_3(\tau)$—we find an extended scaling regime:[31,32]

$$S_q(\tau) \sim S_3(\tau)^{\zeta_q}. \tag{19}$$

Clearly, meaningful results are restricted to the regime in which S_3 is monotonic. For any Gaussian process, the exponents ζ_q follow a simple equation:

$$\zeta_q = 1/3q. \tag{20}$$

Therefore, systematic deviation from the simple scaling relation, Equation 20, should be interpreted as deviation from Gaussianity. An additional remarkable property of the ESS is that it holds rather well, even when the ordinary scaling doesn't exit or can't be detected due to the small scaling range, which is the case for the data analyzed here.

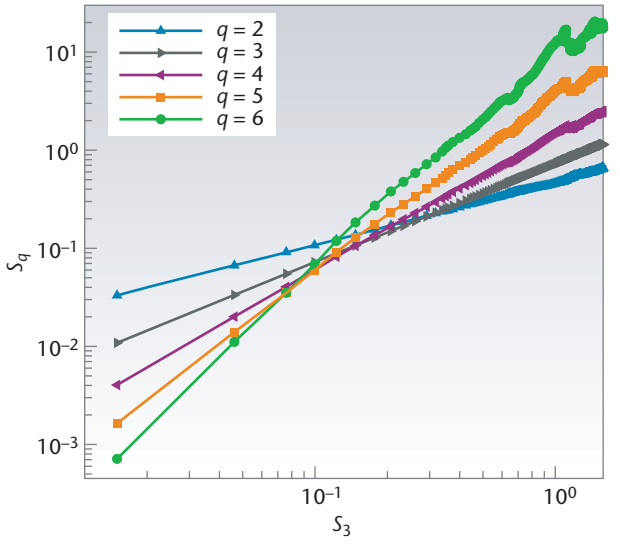

Figure 9. Generalized scaling analysis of a typical healthy subject. The structure functions S_q are displayed versus S_3 in log-log scale.

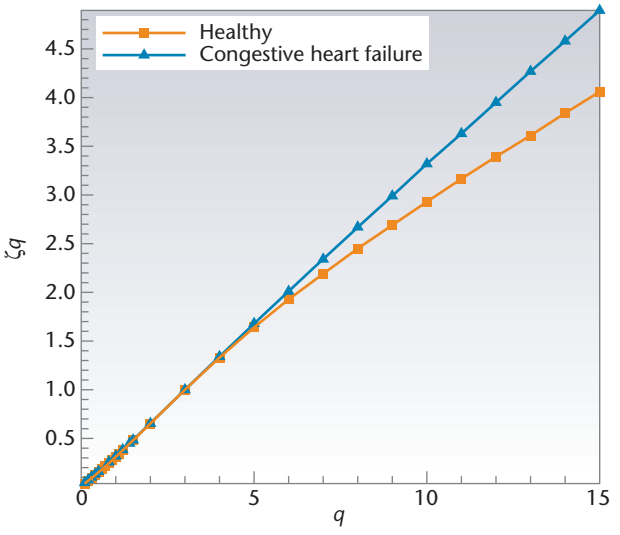

Figure 10. Scaling exponents. The plot of ζ_q versus q varies linearly with q for subjects with congestive heart failure, but has a nonlinear dependence on q for the healthy subjects.

Using the ESS concept, we analyzed[33] the fluctuations in human heartbeat rates of healthy subjects and those with CHF that we looked at earlier with the reconstruction method. Figure 9 shows the results. For a typical healthy subject, the ESS indicates an improved scaling behavior of the time series. In Figure 10, the structure functions' computed scaling exponents ζ_q are plotted against the order q. A monofractal time series corresponds to linear dependence of ζ_q on q, whereas a multifractal time series ζ_q depends nonlinearly on q. The constantly changing curvature of the computed ζ_q for the healthy subjects suggests multifractality of their corresponding time series. In contrast, ζ_q is essentially linear for CHF patients, indicating mono- or simple fractal behavior.

It is well known that the moments with $q < 1$ and $q > 1$ are related to frequent and rare events, respectively, in the time series.[30,31] Thus, for the data considered here, we might also be interested in the frequent events in the interbeats. Figure 11 shows the results for the moment $q = 0.1$ against a third-order structure function for healthy subjects and those with CHF. The figure has two interesting features. First, the starting point of $S_{0.1}(\tau)$ versus $S_3(\tau)$ differs for the healthy subject and CHF patient data. To determine the distance form the origin, we define[34]

$$T(\tau = 1) = [S^2_{0.1}(\tau = 1) + S^2_3(\tau = 1)]1/2. \quad (21)$$

The figure's second important feature is the well-defined τ^* beyond which the plot of $S_{0.1}(\tau)$ versus $S_3(\tau)$ is multivalued. We can estimate τ^* by checking when $S_3(\tau) > S_3(\tau + 1)$. Moreover, if we define $T(\tau^*)$ by

$$T(\tau^*) = [S^2_{0.1}(\tau^*) + S^2_3(\tau^*)]1/2, \quad (22)$$

we get a time scale τ^* such that the third moment's values before and after τ^* are almost the same. Thus, the quantity τ^* plays the role of a local mirror on the time axis. In other words, locally, $S_3(\tau)$ for $\tau < \tau^*$ and $\tau > \tau^*$ have almost the same value. In Figure 11, we show the time scale τ^* and indicate that the interbeat fluctuation values of $T(\tau = 1)$ and $T(\tau^*)$ for healthy subjects and CHF patients differ.

Table 1 presents the computed values of $T_1 = T(\tau = 1)$ for both healthy subjects and those with CHF. To compute the results, we first rescaled the data sets by their standard deviation, so that the T_1 values are dimensionless. The average value of T_1 for the healthy subjects is $\bar{T}(\tau = 1) \simeq 0.5848$, with its standard deviations being $\sigma \simeq 0.065$. The corresponding values for the CHF patients' daytime records are $\bar{T}(\tau = 1) \simeq 0.5077$ and $\sigma \simeq 0.03$, respectively. Therefore, on average, healthy subjects possess T_1 values that are greater than those patients with CHF. Note that the T_1 values for various data sets don't have large enough differences to be able to distinguish the data sets unambiguously. Indeed, as Table 1 indicates, three of the data sets overlap (two belong to two healthy subjects' daytime records and one belongs to one of those subject's nighttime records).

To develop a more definitive criterion for distinguishing the data for various subjects, we can compute values of $T(\tau^*)$. Table 2 shows the results. In this case, it's evident that the data sets have no overlap. Indeed, the healthy subjects' $T(\tau^*)$ values are larger than CHF patients, by a factor of about 3, thus providing an unambiguous way of distinguishing the data sets for healthy subjects and those with CHF.

Comparison with other Methods

Stanley and colleagues[5,13,19,26,27] and other researchers[35–38] have used different methods to analyze the type of data we consider in this review. Their analyses indicate that long-range correlations could exist in the data, characterized by self-affine fractal distributions such as the fractional Brownian motion, the power spectrum of which is given by

$$S(f) \sim f^{-(2H+1)}, \tag{23}$$

where H is the Hurst exponent that characterizes the type of correlations in the data. Thus, healthy subjects are distinguished from those with CHF in terms of the type of correlations that might exist in the data: negative or antipersistent correlations in the increments for $H < 1/2$, as opposed to positive or persistent correlations for $H > 1/2$, and Brownian motion for $H = 1/2$. Although this is an important and interesting result, it can also be ambiguous and not very precise. Suppose the analysis of two time series yields two values of H, one slightly larger and the second slightly smaller than 1/2. It's thus difficult to state with confidence that the two times series are really distinct.

The reconstruction method described earlier analyzes the data in terms of the Markov processes' properties. As a result, it distinguishes the data for healthy subjects from those with CHF in terms of the differences between an FP equation's drift and diffusion coefficients. Such differences are typically significant and thus provide (in our view) an unambiguous way of understanding the differences between the two groups of subjects, including for those series for which the Hurst exponents are only slightly different. In addition, the computational approach described here provides an unambiguous way of reconstructing the data, hence it provides a means of predicting the data's behavior over periods of time that are on the order of their Markov time scales.

Although it remains to be tested, we believe that, together, all the computational methods we've described here are more sensitive to small differences in the data for the two groups and thus might eventually provide a diagnostic tool

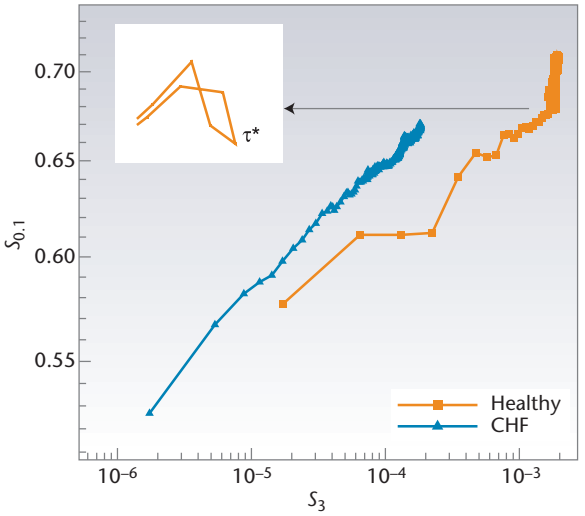

Figure 11. Plot of $S_{0.1}$ against $S_3(\tau)$ for a healthy subject and one with congestive heart failure (CHF). The results indicate that the starting points differ for healthy subjects and those with CHF. Moreover, both data sets have a well-defined τ^* at which $S_3(\tau) > S_3(\tau + 1)$.

Table 1. Values of T_1 for healthy patients and those with congestive heart failure (CHF).

Healthy	CHF
0.658	0.557
0.672	0.565
0.614	0.539
0.605	0.526
0.583	0.512
0.581	0.493
0.576	0.492
0.558	0.481
0.494	0.469
0.480	0.443

Table 2. Values of the $T(\tau^*)$ for healthy patients and for those with congestive heart failure (CHF).

Healthy	CHF
3.08	0.741
2.68	0.714
2.34	0.685
1.92	0.681
1.86	0.675
1.42	0.632
1.40	0.573
1.22	0.728
1.20	0.552
1.15	0.465

WRITE FOR US!

Are you interested in contributing to this department? If so, please contact one of the department editors, Dietrich Stauffer, stauffer@thp.uni-koeln.de, or Muhammad Sahimi, moe@iran.usc.edu.

for early detection of CHF in patients. The computational approaches described here are quite general and could be used for analyzing times series that represent the dynamics of completely unrelated phenomena. We've already used the Markov process concept and extended self-similarity to develop[34] a method for providing short-term alerts for moderate and large earthquakes, as well as making predictions for the price of oil.[39]

References

1. M.F. Shlesinger, "Behavioral-Independent Features of Complex Heartbeat Dynamics," *Ann. New York Academy of Science*, vol. 504, 1987, pp. 214–267.
2. J.B. Bassingthwaighte, L.S. Liebovitch, and B.J. West, *Fractal Physiology*, Oxford Univ. Press, 1994.
3. M. Malik and A.J. Camm, eds., *Heart Rate Variability*, Futura, 1995.
4. M. Kobayashi and T. Musha, "1/*f* Fluctuation of Heartbeat Period," *IEEE Trans. Biomedical Eng.*, vol. 29, 1982, pp. 456–461.
5. J.M. Hausdorff et al., "Fractal Dynamics of Human Gait-Stability of Long-Range Correlations in Stride Interval Fluctuations," *J. Applied Physiology*, vol. 80, 1996, pp. 1448–1454.
6. S.B. Lowen, L.S. Liebovitch, and J.A. White, "Fractal Ion-Channel Behavior Generates Fractal Firing Patterns in Neuronal Models," *Physical Rev. E*, vol. 59, 1999, pp. 5970–5980.
7. Y. Yamamoto et al., "An Indication of Deterministic Chaos in Human Heart Rate Variability at Simulated Extreme Altitude," *Biological Cybernetics*, vol. 69, 1993, pp. 205–211.
8. J.K. Kanters, N.H. Holstein-Rathlou, and E. Agner, "Lack of Evidence for Low-Dimensional Chaos in Heart Rate Variability," *J. Cardiovascular Electrophysiology*, vol. 5, 1994, pp. 128–137.
9. J. Kurths et al., "Complexity Measures for the Analysis of Heart Rate Variability," *Chaos*, vol. 5, 1995, pp. 88–96.
10. P.Ch. Ivanov et al., "Scaling Behaviour of Heartbeat Intervals Obtained by Wavelet-Based Time-Series Analysis," *Nature*, vol. 383, 1996, pp. 323–326.
11. G. Sugihara et al., "Nonlinear Control of Heart Rate Variability in Human Infants," *Proc. Nat'l Academy of Sciences USA*, vol. 93, 1996, pp. 2608–2614.
12. C.-S. Poon and C.K. Merrill, "Decrease of Cardiac Chaos in Congestive Heart Failure," *Nature*, vol. 389, 1997, pp. 492–494.
13. P.Ch. Ivanov et al., "Multifractality in Human Heartbeat Dynamics," *Nature*, vol. 399, 1999, pp. 461–464.
14. M. Mackey and L. Glass, "Oscillation and Chaos in Physiological Control Systems," *Science*, vol. 197, 1977, pp. 287–290.
15. M.M. Wolf et al., "Sinus Arrhythmia in Acute Myocardial Infarction," *Medical J. Australia*, vol. 2, 1978, pp. 52–67.
16. R.I. Kitney and O. Rompelman, *The Study of Heart-Rate Variability*, Oxford Univ. Press, 1980.
17. S. Akselrod et al., "Power Spectrum Analysis of Heart Rate Fluctuation: A Quantitative Probe of Beat-to-Beat Cardiovascular Control," *Science*, vol. 213, 1981, pp. 220–224.
18. C.-K. Peng et al., "Quantification of Scaling Exponents and Crossover Phenomena in Nonstationary Heartbeat Time Series," *Chaos*, vol. 5, 1995, pp. 82–87.
19. Y. Ashkenazy et al., "Magnitude and Sign Correlations in Heartbeat Fluctuations," *Physical Rev. Letters*, vol. 86, 2001, pp. 1900–1903.
20. R. Friedrich and J. Peinke, "Description of a Turbulent Cascade by a Fokker-Planck Equation," *Physical Rev. Letters*, vol. 78, 1997, pp. 863–866.
21. J. Davoudi and M.R. Rahimi Tabar, "Theoretical Model for the Kramers-Moyal Description of Turbulence Cascades," *Physical Rev. Letters*, vol. 82, 1999, pp. 1680–1683.
22. G.R. Jafari et al., "Stochastic Analysis and Regeneration of Rough Surfaces," *Physical Rev. Letters*, vol. 91, 2003, pp. 226101/1–226101/4.
23. R. Friedrich, J. Peinke, and C. Renner, "How to Quantify Deterministic and Random Influences on the Statistics of the Foreign Exchange Market," *Physical Rev. Letters*, vol. 84, 2000, pp. 5224–5227.
24. M. Siefert et al., "On a Quantitative Method to Analyze Dynamical and Measurement Noise," *Europhysics Letters*, vol. 61, 2003, pp. 466–469.
25. M. Ragwitz and H. Kantz, "Indispensable Finite Time Corrections for Fokker-Planck Equations from Time Series Data," *Physical Rev. Letters*, vol. 87, 2001, pp. 254501/1–254501/4.
26. P.Ch. Ivanov et al., "Sleep-Wake Differences in Scaling Behavior of the Human Heartbeat: Analysis of Terrestrial and Long-Term Space Flight Data," *Europhysics Letters*, vol. 48, 1999, pp. 594–598.
27. Y. Ashkenanzy et al., "Noise Effects on the Complex Patterns of Abnormal Heartbeats," *Physical Rev. Letters*, vol. 87, 2001, pp. 068104/1–068104/4.
28. F. Ghasemi et al., "Regeneration of Stochastic Processes: An Inverse Method," *European Physical J. B*, vol. 47, 2005, pp. 411–415.
29. F. Ghasemi et al., "Statistical Properties of the Interbeat Interval Cascade in Human Hearts," to be published in *Int'l J. Modern Physics C*, 2005.
30. T. Kuusela, "Stochastic Heart-Rate Model Can Reveal Pathologic Cardiac Dynamics," *Physical Rev. E*, vol. 69, 2004, pp. 031916/1–031916/5.
31. R. Benzi et al., "Scaling Property of Turbulent Ows," *Physica D*, vol. 96, 1996, pp. 162–168.
32. A. Bershadskii and K.R. Sreenivasan, "Extended Self-Similarity of the Small-Scale Cosmic Microwave Background Anisotropy," *Physics Letters A*, vol. 319, 2003, pp. 21–24.
33. F. Ghasemi et al., "The Extended Self-Similarity of Interbeat Intervals in Human Subjects," to be published in *J. Statistical Mechanics Theory and Experiment*, 2006.
34. M.R. Rahimi Tabar et al., "Dynamics of the Markov Time Scale of Seismic Activity May Provide a Short-Term Alert for Earthquakes," to be published in *Geophysical Research Letters*, 2006.
35. R.G. Turcott and M.C. Teich, "Fractal Character of the Electrocardiogram: Distinguishing Heart-Failure and Normal Patients," *Ann. Biomedical Eng.*, vol. 24, 1996, pp. 269–275.
36. L.A. Lipsitz et al., "Spectral Characteristics of Heart Rate Variability Before and During Postural Tilt: Relations to Aging and Risk of Syncope," *Circulation*, vol. 81, 1990, pp. 1803–1808.
37. N. Iyengar et al., "Age-Related Alterations in the Fractal Scaling of Cardiac Interbeat Interval Dynamics," *Am. J. Physiology*, vol. 271, 1996, pp. R1078–R1083.
38. P.Ch. Ivanov et al., "Stochastic Feedback and the Regulation of Biological Rhythms," *Europhysics Letters*, vol. 43, 1998, pp. 363–368.

39. F. Ghasemi et al., "The Kramers-Moyal Expansion and Langevin Equation for the Stochastic Fluctuations in the Oil Price," submitted to *Physical Rev. Letters*, 2005.

Mohammad Reza Rahimi Tabar is an associate professor of physics at Sharif University in Tehran, Iran. His main research areas are conformal field theory, disordered systems, statistical theory of turbulence, stochastic processes, seismic activity, and wave localization. Contact him at rahimitabar@sharif.edu.

Fatemeh Ghasemi is a postdoctoral fellow at the Institute for Studies in Theoretical Physics and Mathematics in Tehran, Iran. Her main research interests are stochastic processes, analysis of time series and of rough surfaces, and seismic activity. Contact her at f_ghasemi@mehr.sharif.edu.

Joachim Peinke is a professor at the University of Oldenburg, Germany. His main research areas are turbulence, econophysics, pattern formation in nematic liquid crystals, stochastic processes, and development of various sensors. Contact him at peinke@uni-oldenburg.de.

Rudolf Friedrich is a professor at the University of Münster, Germany. His main research areas are turbulence, econophysics, pattern formation in nematic liquid crystals, and stochastic processes. Contact him at fiddir@uni-muenster.de.

Kamran Kaviani is an assistant professor of physics at Alzahra University in Tehran, Iran. His main research interests are stochastic processes and field theory. Contact him at kaviani@yahoo.com.

Fatemeh Taghavi is a PhD student at the Iran University of Science and Technology in Tehran, Iran. Her main research interests are stochastic processes and field theory. Contact her at f_taghavi@iust.ac.ir.

Sara Sadeghi is a PhD student at Sharif University in Tehran, Iran. Her main research area is analysis of complex systems. Contact her at s_sara2001@yahoo.com.

Golnoosh Bizhani is pursuing an MSc in physics at Sharif University in Tehran, Iran. Her main research area is analysis of complex systems. Contact her at golnoosh_bizhani@yahoo.com.

Muhammad Sahimi is a professor of chemical engineering and materials science and the NIOC Professor of Petroleum Engineering at the University of Southern California, Los Angeles. His main research areas are atomistic simulation of nanostructured materials, modeling of large-scale porous media, wave propagation in heterogeneous media, and analysis of stochastic processes. Contact him at moe@iran.usc.edu.